Journal of Polymer Research (2022) 29: 372
https://doi.org/10.1007/s10965-022-03219-8

ORIGINAL PAPER

Gamma irradiation synthesis of pectin- based biohydrogels for removal of lead cations from simulated solutions

Asmaa Sayed[1] · Fatma Hany[2] · Manar El-Sayed Abdel-Raouf[3] · Ghada A. Mahmoud[1]

Received: 9 March 2022 / Accepted: 28 July 2022 / Published online: 9 August 2022

Abstract

Bio-based hydrogels (denoted as PC-PAAc/GA) comprised of Pectin (PC) and polyacrylic acid (PAAc) reinforced with different ratios of gallic acid (GA) were prepared by gamma radiation at irradiation dose 20 kGy. The prepared hydrogels were investigated by different analytical tools. The swelling performance was studied versus time, pH of the medium and gallic acid content. The experimental data depicted that the swelling increases with pH of medium until the equilibrium of swelling after 350 min. The maximum swelling was attained at pH10 for both PC-PAAc and PC-PAA/GA1.5. Also, the data reveal that the incorporation of GA in the hydrogel matrix enhanced the swelling performance of the hydrogel up to an optimum value of GA, i.e. PC-PAA/GA1.5. Further increase in GA concentration leads to formation of a highly crosslinked structure with reduced swelling. The results demonstrated that the prepared hydrogels displayed excellent antibacterial activity against gram + ve bacteria *(E.coli)* and gram-ve bacteria *(S.aureus)*. This potent antimicrobial activity is mainly originated from GA which was proved as a strong antibacterial agent. Moreover, the removal performance of the investigated hydrogels was verified towards Pb^{+2} cation as one of the most poisonous heavy metals. The data revealed that the maximum removal percentage of Pb (II) was attained by PC-PAAc/GA1.5 hydrogel (90 mg g^{-1}). The correlation coefficients of the Langmuir model are too higher than that of the Freundlich model that assumed the adsorption of lead cations is mainly a chemical process.

Keywords Atomic force microscope · Gallic acid · Gamma-irradiation · Pectin · Polyacrylic acid · Removal metal cations

Introduction

The remediation of polluted water has gained prodigious global attention [1–5]. Indeed, numerous contaminants produced from different human activities are discharged into water effluents [6, 7]. The sources of heavy metal cations in running water include the sewage of the industrial factories, agricultural pesticide wastes, and metal mining [8]. Certain heavy metal ions such as lead, mercury, and arsenic are highly hazardous as they induce a series of threats to the entire ecosystem; and specially to the food chain from the base to the top [9, 10]. There were numerous solutions proposed by several researchers to eliminate different heavy metals, or at least to reduce their destructive effects [11–13].

Most of the commonly used techniques are chemically based, such as precipitation, electro-dialysis, or oxidation and reductions reactions [14]. Other physical protocols such as ultrafiltration are also applied [15].

Adsorption technology has been employed as one of the most promising techniques for heavy metal ions removal [16, 17]. Among different adsorbents, hydrogels are considered very attractive materials [18, 19]. Hydrogels contain active groups such as $-COOH$, $-OH$, and $-NH_2$ in their network structures, which are necessary for the chelating of the heavy metal ions [20]. Bio-based hydrogels are considered a green alternative to traditional hydrogels [21, 22]. The properties of natural polymers have shed light on their reputation in several fields [23–26]**.** Pectin is a hydrophilic polysaccharide that occurs naturally and is increasingly used in the pharmaceutical and biotechnology industries [27, 28]. It is inexpensive, biodegradable, biocompatible, and renewable, thus encouraging researchers to investigate its possible use

✉ Ghada A. Mahmoud
ghadancrrt@yahoo.com

[1] Polymer Chemistry Department, National Center for Radiation Research and Technology, Egyptian Atomic Energy Authority, Cairo, Egypt

[2] Faculty of Biotechnology, October University for Modern Sciences and Arts (MSA), 6th of October, Egypt

[3] Egyptian Petroleum Research Institute, 1Ahmed Elzomor Street, 11727, Nasr city, Cairo, Egypt

in industrial applications [29–31]. However, the low chemical resistance and microbial attack limit industrial applications of pectin. It can be overcome by copolymerization with a synthetic polymer such as polyacrylic acid (PAAc) [32]. Copolymers offer benefits not usually noticed in homopolymers [33]. So, most absorbable polymers are of copolymer types. Poly(acrylic acid) grafted pectin and cross-linked with glutaraldehyde was investigated in the adsorption of cadmium ions [34].

Gallic acid (GA) (3, 4, 5-trihydroxybenzoic acid) is a naturally occurring low molecular weight trihydroxy molecule with potent antioxidant properties. It is found in many foods such as grapes, nuts, tea, and sumac in its free form or as one of its derivatives. GA exists as an ester in plant tissues, and several esters of sugars, glycosides, polyols, and phenols have also been identified [35]. It effectively protects against oxidative damage caused by reactive species such as superoxide (O_2), hydroxyl (HO^-), and peroxyl (ROO^-), as well as non-radicals such as hypochlorous acid (HOCl) and hydrogen peroxide (H_2O_2), which are often encountered in biological systems [36]. On the other hand, radiation induced crosslinking has been widely known for its readiness and greenness [37, 38].

The current study presents the preparation of a new series of eco-friendly hydrogels based on Pectin-Poly (acrylic acid)/gallic acid (PC-PAAc/GA) via gamma irradiation technique. The prepared hydrogels are investigated under different working conditions to verify their suitable usability as effective sorbents. The elements of the claimed hydrogels were carefully selected to achieve maximum removal performance. For instance, the carboxylic acid groups of Pectin and PAAc display high activity towards metal ions via chelation. The incorporation of GA in the hydrogel matrix is due to its antibacterial activity which is crucial for safe wastewater treatment. Compared with chemical methods, preparing hydrogels by radiation-induced copolymerization is a clean, convenient, and inexpensive method [39–41]. The prepared bio-based hydrogels were inspected as possible adsorbents for the removal of Pb(II) ions from simulated solutions.

Materials and methods

Chemicals

Pectin powder (PC) extracted from apple peels, with a degree of esterification of 50–75%, was purchased from Sigma-Aldrich (China). Acrylic acid (AAc), purity of 99.9%, was supplied from Aldrich, Darmstadt, Germany. Gallic acid (GA) was obtained from Qualikems Fine Chem Pvt (India). Other chemicals such as NaOH, HCl and $Pb(NO_3)_2$ were purchased from El-Nasr Co. (Cairo, Egypt) as high grade chemicals. Deionized water was used in all the experiments.

Preparation of PC-PAAc/GA hydrogel

5 g of pectin was dissolved in 65 mL of deionized water and stirred at 60 °C until obtaining a homogenous solution. Then 30 mL of AAc monomer was added to the pectin solution, and the mixture of PC-AAc was stirred on a magnetic stirrer at ambient temperature until homogeneity, where the total polymer/monomer content was 35 wt%. 2 g of GA was added to 50 mL of distilled water and was sonicated at 25 °C for 30 min. The mixture was stirred on a magnetic stirrer until GA was fully dissolved. Different volumes of GA solution (mL), 0.0, 0.5, 1.0, 1.5, and 2.0, were added to the prepared PC-AAc solution (where the total volume of each was 20 mL) with continuous stirring (Table 1). The resulted solutions were poured into glass test tubes, and they were exposed to ^{60}Co-gamma irradiation at an irradiation dose of 20 kGy. The produced hydrogels were sliced into almost identical discs. Then, the discs were extracted in distilled water at 70 °C for two hours to exclude the unreacted materials and air-dried to a constant weight.

Characterization of PC-PAAc/GA hydrogels

Fourier transform infrared spectroscopy (FT-IR)

The IR spectra of PC-PAAc/GA hydrogels were recorded on FT-IR model Bruker, Unicom infra-red spectrophotometer, Germany, at 400–4000 cm^{-1} wavelength range.

X–ray diffraction analysis (XRD)

The crystallinity of PC-PAAc/GA hydrogel samples was examined at room temperature by XD-DI Series, Shimadzu device containing copper target with ($\lambda = 1.542$ Å), 30 mA electric current, 40 kV operating voltage, over 2θ of range

Table 1 The composition of different PC-AAc/ GA formulations

Sample	PC-AAc (mL)	PC-AAc (wt.%)	GA (mL)	GA (wt.%)
PC-PAAc/GA0	20.0	1	0.0	0
PC-PAAc /GA0.5	19.5	0.975	0.5	0.02
PC-PAAc /GA1	19.0	0.950	1.0	0.04
PC-PAAc /GA1.5	18.5	0.925	1.5	0.06
PC-PAAc /GA2	18.0	0.900	2.0	0.08

4° to 90°, and speed of scanning 8°/min to measure the X-Ray Diffraction (XRD) patterns of the samples.

Thermogravimetric analysis (TGA)

TGA was carried out using a thermogravimetric analyzer (Perkin-Elmer Co., USA) at a heating rate of 15◦C $min^{-1}$from 30 to 600◦C under a nitrogen atmosphere.

Atomic force microscopy (AFM)

The topography of PC-PAAc /GA dry, wet hydrogels, and metal loaded were monitored via the AFM, Flexaxiom Nanosurf, C3000 at the dynamic mode (non-contact) to confirm chemical modification and to detect the changes accompanying the removal process. The AFM examinations were conducted at room temperature using a NCLR rectangular-shaped silicon cantilever with a resonant frequency of 9 kHz.

Field emission scanning electron microscopy (FE-SEM)

The surface morphology of PC-PAAc /GA dry, wet hydrogels, and metal loaded were monitored via a high-resolution electron microscope (SEM) (JEOL—JSM 5200 SCANNING MICROSCOPE, Japan) with voltage accelerated at 25 kV.

Swelling study

A hydrogel disc of known weight was submerged in 30 mL distilled water at different time intervals till reaching the equilibrium state. The extra water on the turgid sample's surface was removed using a filter paper then the samples were reweighed again. The swelling percentage was calculated using the following equation:

$$\text{Swelling}\,(\%) = \frac{W_t - W_d}{W_d} \times 100 \quad (1)$$

where, W_t is the weight of the wet hydrogel at time "*t*" and W_d is weight of dry hydrogel.

To study the effect of pH on the swelling behavior, a known weight of PC-PAAc/GA1.5 and Pectin/PAAc/GA0 hydrogels was immersed in buffer solutions at pH's 2, 3, 5.5, 7.5, and 10.5 at room temperature for 350 min. The above steps were repeated to calculate the swelling percent.

Antibacterial activity assessment

Antibacterial activity against *Escherichia coli (E.coli)* ATCC 25,922 (a representative Gram-negative bacterium) and *Staphylococcus aureus subsp. aureus (S.aureus)* ATCC 25,923 (a representative Gram-positive bacterium) was examined using the agar diffusion method described in AATCC TM 147–1998 [42]. The sample with a diameter of around 0.5 cm was sterilized by UV irradiation for 15 min on both sides and gently placed onto the agar surface. After the incubation at 37 °C for 24 h, a clear area indicating no bacterial growth along the borders of the sample or antagonistic zone was measured and recorded. Each sample was measured three times.

Adsorption study

The batch equilibrium technique was used to study the adsorption behavior of the prepared hydrogels towards Pb(II) ions. In this regard, 0.05 g of the hydrogel sample was immersed in 20 mL of Pb(II) cation solution of initial concentration of 50 mg/L (C_0) at ambient temperature (~25 °C) and pH = 5 with stirring for 24 h. Then the hydrogel was removed, and the final concentration of Pb(II) ions (C_f mg/L) was measured using Agilent 5100 Inductively Coupled Plasma -Optical Emission Spectrophotometer (ICP-OES) with Synchronous Vertical Dual View (SVDV). For each series of measurements, the intensity calibration curve was constructed composed of a blank and three or more standards from Merck. The standard reference material for trace elements in water and quality control samples from the National Institute of Standards and Technology (NIST), was used to confirm the instrument readings.

The removal percentage was calculated using the following equation [43]:

$$\text{The removal}\,(\%) = \frac{C_0 - C_f}{C_0} \times 100 \quad (2)$$

In order to investigate the adsorption isotherms, the effect of Pb(II) ions concentration on the removal percentage was studied using different concentrations of Pb(II) ions; 10, 20, 30, 50, 70, and 100 mg/L. In each experiment, 0.05 g of PC-PAAc/GA0 and PC-PAAc/GA1.5 hydrogels were placed in 20 mL of Pb(II) ions of a definite concentration for 24 h with stirring at ambient temperature (~25 °C). The previous steps were repeated and the removal (%) was calculated using Eq. (2).

Reusability study

The reusability of the most effective sorbent was investigated at three swelling/deswelling cycles. The composites were immersed in HCl (1 M, 30 mL) solution with a magnetic stirrer at room temperature for 60 min to remove all the sorbet material and to clean the adsorbent for further removal.

Statistical analysis

The prepared hydrogel properties were estimated in triplicate as the replicated experimental units, The data were plotted using Origin 2016 (OriginLab Corp., Northampton, MA, USA), and all the results were statistically analyzed using the ONE-WAY ANOVA. Differences among average values were analyzed by Duncan's multiple range tests using IBM SPSS software version 24 as a statistical resource at $P < 0.05$.

Results and discussion

Preparation of the hydrogel

Gamma irradiation is efficient and simple technique for the preparation of hydrogel. When the solution mixture PC polymer and AAc monomer is subjected to gamma rays, radiolysis of water during irradiation yields hydrogen (H·) and hydroxyl (OH·) free radicals. The (OH·) attack the polymer chain to form a macroradical. The free radicals formed on AAc start to polymerize. The macroradicals attack the AAc moieties to produce a crosslinked network structure of PC-PAAc hydrogel. GA molecule can interact with PC to form PC-PAAc /GA hydrogel product, as shown in Fig. 1. A fixed dose of gamma (20KGy) irradiation was applied to promote crosslinking based on previous studies to obtain the desirable degree of crosslinking. It is established that high irradiation doses induce formation of highly crosslinked structures with undesired properties [44–46].

Swelling behavior

Figure 2a shows the swelling behavior of PC-PAAc/GA hydrogels of different GA contents as a function of time. The swelling behavior of a hydrogel is controlled by the main backbone structure that is made up of cross-linked chains [47]. As seen in the Figure PC-PAAc/GA hydrogels displayed high swelling behavior, which was boosted by time until the equilibrium of swelling was attained after 350 min for all hydrogels. On the other hand, it can be noted that the swelling equilibrium increases with increasing GA content in PC-PAAc/GA hydrogel network structure, Fig. 2b. The hydrophilicity of PC-PAAc/GA hydrogels was enhanced by increasing the hydrophilic moieties, which was done by increasing GA content. However, a drop in the swelling equilibrium was observed as the GA content was increased in PC-PAAc/GA2. A higher GA content may produce a denser network structure as well as diminished space for water storage [48]. The high swelling property is an important feature in using material as an adsorbent. The higher the available active sites on the network structure, the higher the swelling will be. Therefore, PC-PAAc/GA1.5 hydrogel was chosen to be used in the following studies where it exhibited the highest swelling (%).

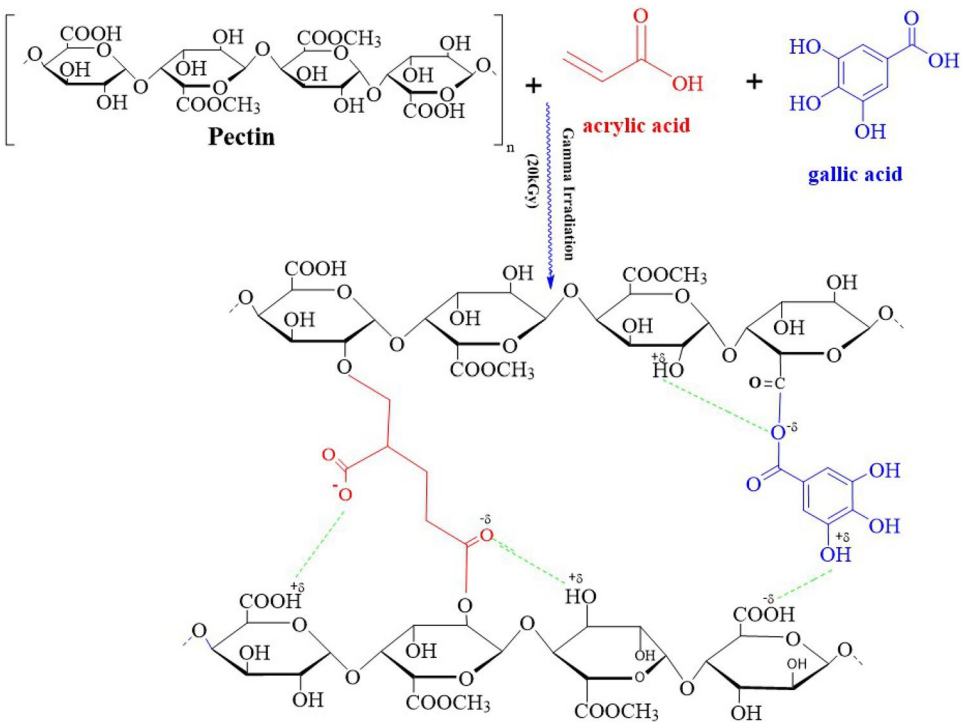

Fig. 1 A proposed reaction for formation of PC-PAAc/GA hydrogel

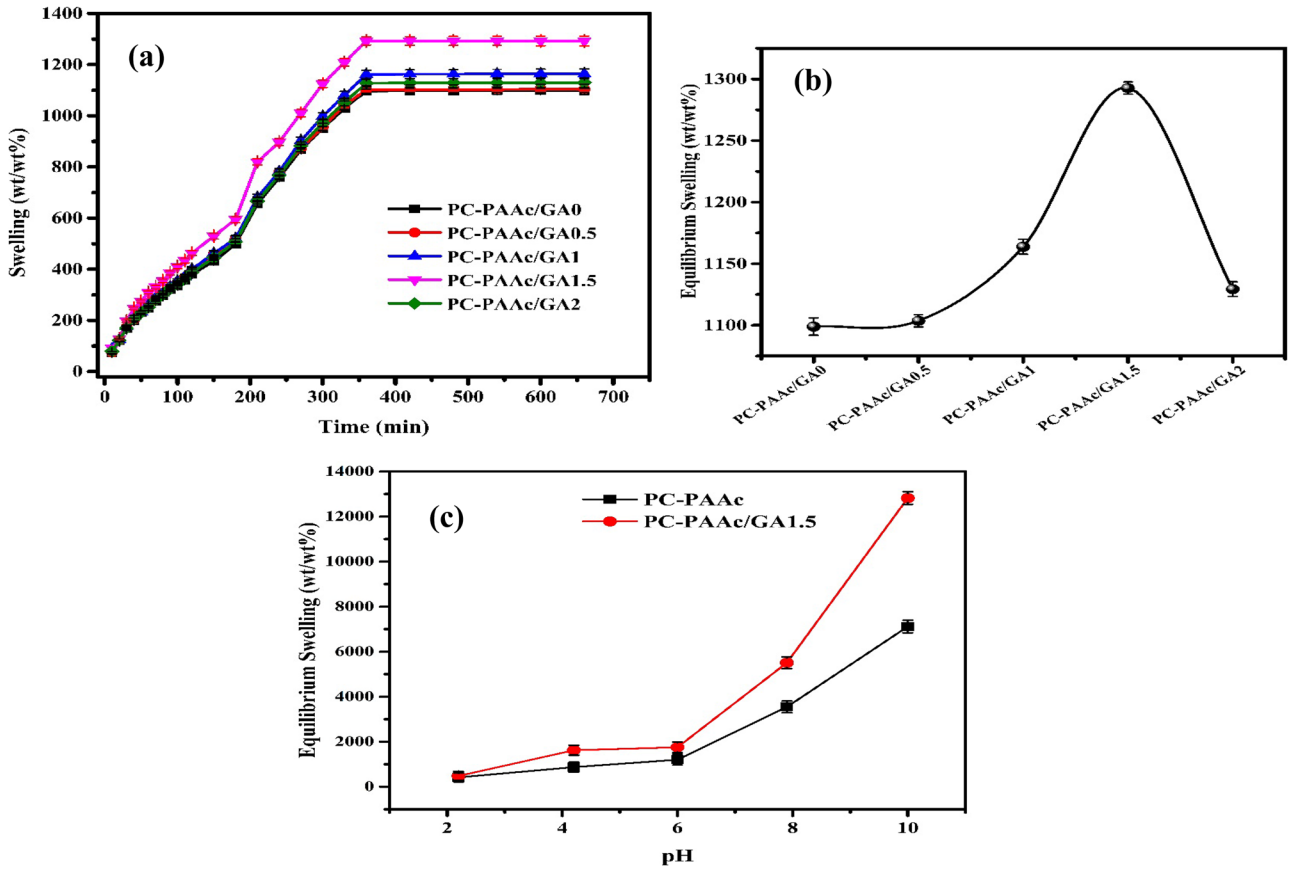

Fig. 2 Swelling behavior of the PC-PAAc/GA hydrogels as a function of time (**a**) GA content (**b**) and pH (**c**)

Figure 2c shows the effect of pH on the equilibrium swelling of PC-PAAc/GA1.5 hydrogel compared with PC-PAAc/GA0. The equilibrium of swelling was enhanced by increasing pH from 2 to 10 for both hydrogels. It is known that the carboxylic group is responsive to the medium pH. The carboxylic group protonates in an acidic medium up to pH; 4.6 where it is the pKa value of PAAc [49]. Therefore, an extra increase in pH value produces deprotonation of the carboxylic group. The repulsion of the negatively charged carboxylate ions permits the uptake of more water molecules, thus enhancing the equilibrium of swelling [42].

Fourier transform infrared spectroscopy analysis (FT-IR)

Figure 3a shows FTIR spectra of PC-PAAc/GA0 and PC-PAAc/GA1.5 hydrogels. In both spectra, there is a wide peak at 3200- 3600 cm^{-1} assigned to O–H groups. The peak of C-H appears at 2937 cm^{-1} in PC-PAAc/GA0 hydrogel. The peaks of aliphatic C-H and aromatic C-H of phenolic rings of GA overlapped with the O–H peak in PC-PAAc/GA1.5 hydrogel spectrum [50]. The peak of C = O was obtained at 1707.7 cm^{-1} for PC-PAAc/GA0, which was shifted to 1710 cm^{-1} by adding GA in the hydrogel matrix. The C-H stretching vibration has been confirmed by the peak at 1448 cm^{-1} for PC-PAAc/GA0 hydrogel and shifted to 1460 cm^{-1}. The peak at 1158 cm^{-1} corresponds to the stretching vibration of $–COO^-$ that reduced and shifted to 1160 cm^{-1} in PC-PAAc/GA1.5 [51, 52]. It is suggested that the intramolecular hydrogen bonds, which are formed between GA and polymeric chain are responsible for shifting and reducing the intensity of peaks of PC-PAAc/GA1.5 hydrogel [53].

X-ray diffraction analysis (XRD)

The XRD patterns of PC-PAAc/GA0 and PC-PAAc/GA1.5 hydrogels is illustrated in Fig. 3a. It is clear that the X-ray diffraction patterns for both hydrogels depicted broad peaks at $2\theta = 20.4°$ that reflected the amorphous structure of the hydrogels [54]. The intensity of this peak increased, and the broadness of the peak decreased after the incorporation of GA in PC-PAAc/GA1.5 hydrogel implied increasing in crystallinity. GA may act as a plasticizer, thus decreasing the activation energy and enabling polymeric chain mobility.

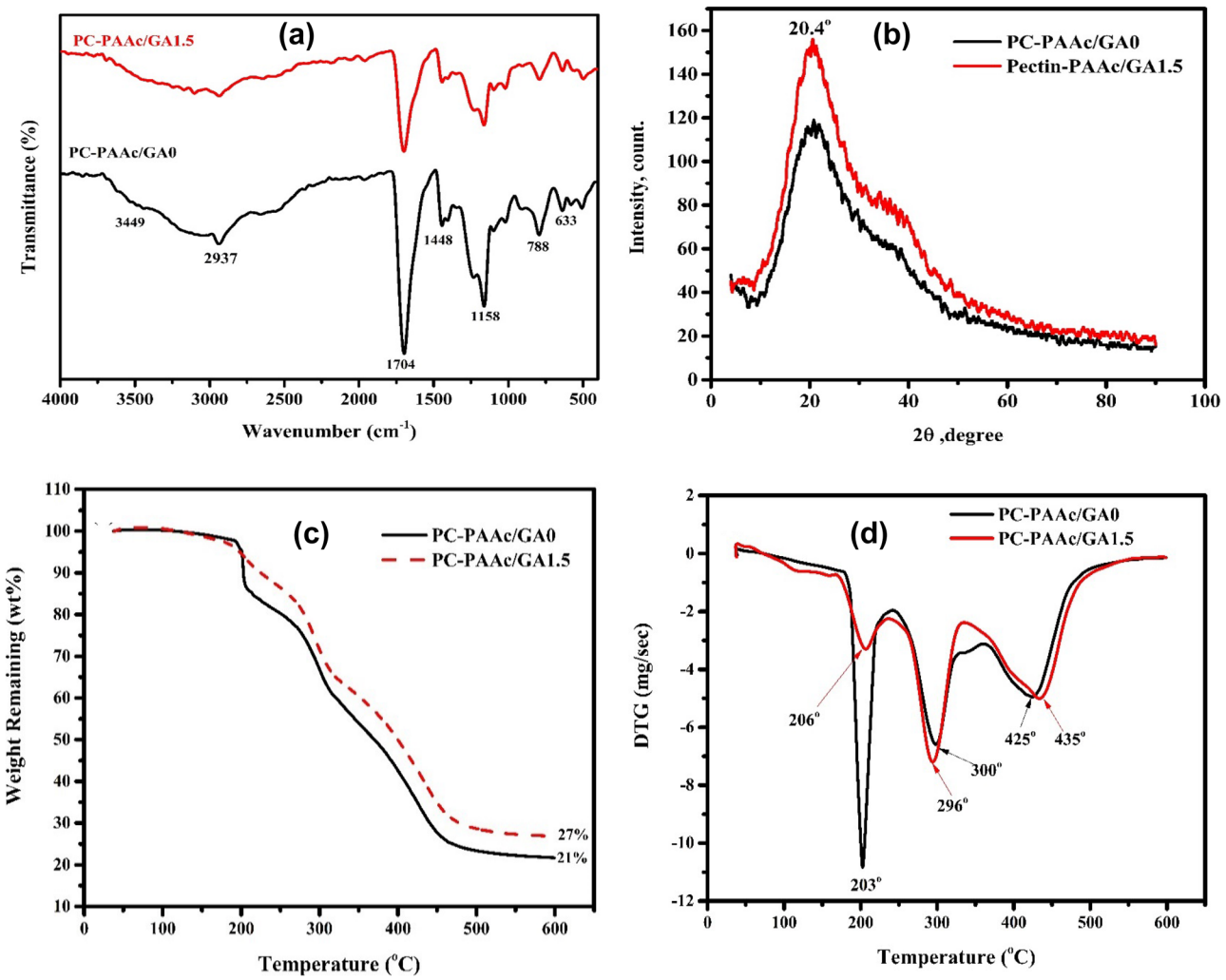

Fig. 3 FTIR spectra (**a**), XRD diffraction patterns (**b**) TGA (**c**) and DTG (**d**) thermograms of PC-PAAc/GA0 and PC-PAAc/GA 1.5 hydrogels

Thermal stability

The thermal stability of PC-PAAc/GA1.5 compared with PC-PAAc/GA0 hydrogel was investigated by TGA and DTG, as shown in Figs. 3c, d. It can be noted that the thermal degradation was performed in three decomposition stages for both hydrogels. The first decomposition stage was shown at 203 °C for PC-PAAc/GA0 and increased to 206 °C for PC-PAAc/GA1.5 hydrogel due to the elimination of the hydrated water. The second decomposition stage appeared at 296 °C and 300 °C C for PC-PAAc/GA0 and PC-PAAc/GA1.5 hydrogels, respectively, due to the elimination of side groups. The third decomposition stage is the main stage where decomposition of the backbone matrix was achieved. The stage was performed at 425 °C for PC-PAAc/GA0 and 435 °C for PC-PAAc/GA1.5 hydrogel. The weight residue of PC-PAAc/GA0 hydrogel is 21% and for PC-PAAc/GA1.5 is 27%. The results indicated that the thermal stability of PC-PAAc/GA1.5 hydrogel is higher than PC-PAAc/GA0. The thermograms proved the higher degradation temperature for PC-PAAc/GA1.5 than PC-PAAc/GA0, assuming the improvement in the thermal stability by adding GA. Similar behavior was obtained by Samper et al. [55], where 0.5 wt % silibinin and quercetin acted as oxidative retardants for PP as both natural additives successfully delayed the onset of thermal oxidation. Dopico-Garcia et al. [56] showed that the use of natural antioxidants could successfully result in polyolefins with enhanced stabilization against thermal-oxidation degradation.

Surface and topography investigations

The AFM images of PC-PAAc/GA0 and PC-PAAc/GA1.5 hydrogels are given in Fig. 4. Upon investigating the provided images, it can be seen that the prepared hydrogels are

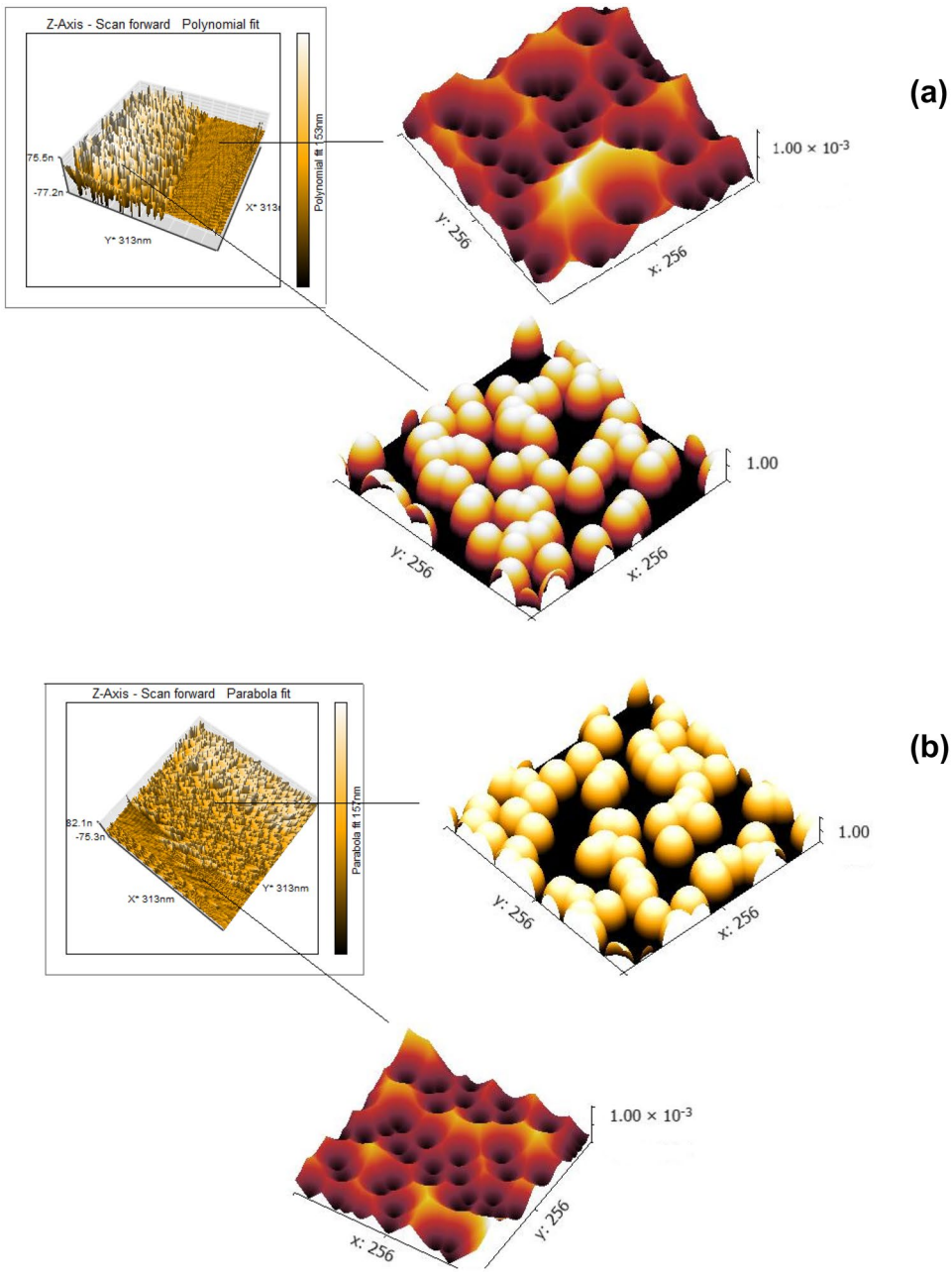

Fig. 4 AFM images of PC-PAAc/GA0 (**a**) and PC-PAAc/GA1.5 (**b**) hydrogels

highly porous with a rough surface. The effect of structural variation on the topography and the roughness of the prepared hydrogels is clear. The incorporation of GA in the hydrogel matrix improved the porous and roughness of the surface.

Antibacterial activity

The antibacterial activity of PC-PAAc/GA1.5 hydrogel compared with PC-PAAc/GA0 against gram + bacteria *(E. coli)* and gram- bacteria *(S.aureus)* was investigated as shown in Fig. 5. It can be observed that there is a clear inhibition zone surrounding PC-PAAc/GA1.5 against *E. coli* and *S.aureus* (Fig. 5b, d), where it does not exist in PC-PAAc/GA0 hydrogel that is gallic acid-free. The clear large inhibition zone for PC-PAAc/GA1.5 hydrogel reflected a successful inhibiting against the bacterial growth for both gram^{+} and gram^{-}, and confirming the strong antimicrobial activity of GA. The results proved that the prepared hydrogel has excellent antibacterial properties, and the antibacterial activity mainly originated from GA. Since the GA molecule is a benzoic acid derivative, it contains three hydroxyl groups. It is considered that the more the acid includes hydroxyl groups, the

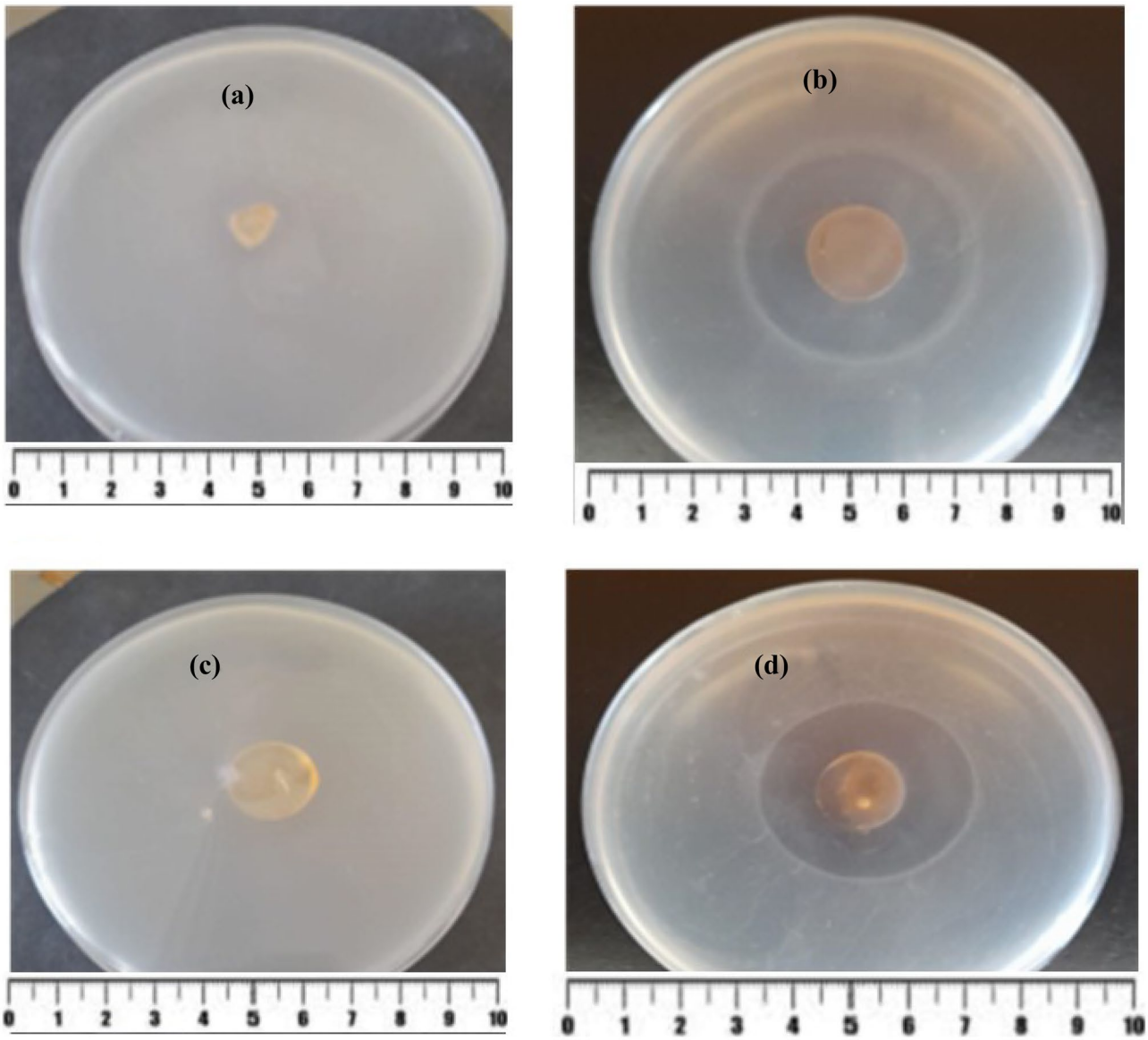

Fig. 5 Photographs of the inhibition zone of the PC-PAAc/GA0 against gram + bacteria (**a**), gram- bacteria (**c**) and PC-PAAc/GA1.5 against gram + bacteria (**b**), gram- bacteria (**d**)

better the antimicrobial activity will have. These acids are attacking the microorganism due to the antioxidant property of the phenolic compounds. The more the hydroxylation and the antioxidant concentration, the high the toxicity that kills the microorganisms. The COOH groups and the H-donating have significant capabilities to stabilize free radicals. The GA molecule is rupturing the bacterial cell wall. It works by disturbing the permeability of the cell membrane and preventing the formation of a bacterial biofilm. Similar investigation was proven by Miklasińska-Majdanik et al. [57].

Adsorption study

In this section, the capability of the prepared PC-PAAc/GA hydrogels towards the removal of Pb (II) ions was investigated. Figure 6 shows the effect of GA content in the hydrogel matrix on the removal of Pb (II) ions. The investigation was performed at initial metal ions concentration; 50 mg/L and at the pH of the Pb (II) ions solution = 5. It should be noted that above pH 5.5, insoluble lead hydroxide precipitated thus, the adsorption investigation was failed [58]. At the same time, the carboxylic groups on the hydrogel

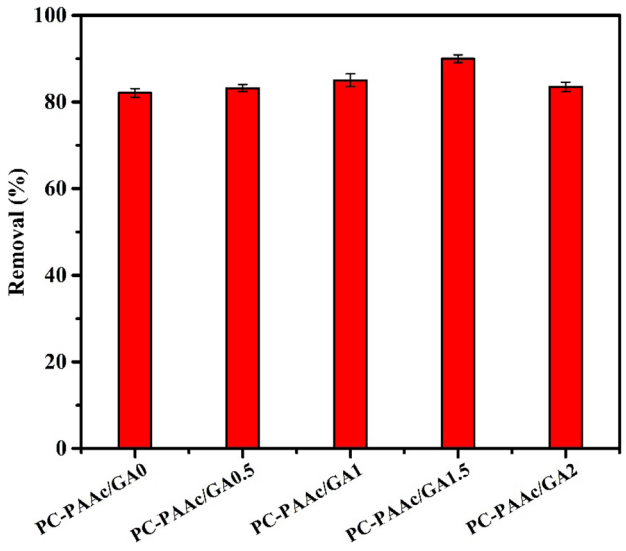

Fig. 6 Effect of GA content on removal (%) of Pb(II) by PC-PAAc/GA hydrogels at initial metal concentration 50 mg/L, time 24 h and,adsorbate weight 0.05 g

deprotonated above 4.6 as mentioned before. Therefore, the pH of Pb (II) ions solution does not need any adjustment. As seen in Fig. 6, no remarkable increase in the removal (%) was observed by increasing GA content. The removal percentage of Pb (II) ions by PC-PAAc/GA0 is 82.1 was increased by increasing GA content to get the maximum value of 90% by using Pectin-PAAc/GA1.5. A drop in the removal (%) to 83.5 was noticed by applying PC-PAAc/GA2.

An interesting investigation for studying the surface changes of PC-PAAc/GA hydrogels after the uptake of Pb (II) ions is shown in Fig. 7a–j. The obtained images demonstrated the efficiency of the AFM in monitoring the surface variation, describing the changes associated with the removal process, and confirming the affinities of the hydrogels towards Pb (II). Upon investigating the provided images, it can be seen that the prepared hydrogels are highly porous with a rough surface. Although there are no noticeable changes in the height values, there is a visible change in roughness measurement, which increases by the increase in GA content in the hydrogel matrix, as seen in Fig. 7k, l. The images and the derived AFM data run parallel to the swelling data and prove that the maximum removal performance was achieved by PC-PAAc/GA1.5 hydrogel. It can be concluded that the roughness and height measurements increase as the porosity increases, i.e. as the order of increasing the amount of GA. However, a decrease in roughness and height for PC-PAAc/GA2 was observed. Further increase of GA content causes blockage of pores and diminishing of pore volume, which leads to a reduction in the height and roughness and negatively affects the removal efficiency. This finding may be attributed to the benzene ring of GA, which decreases the hydrophilicity and therefore reduces the metal uptake. Our finding agrees with Zhang et al. and Gray et al. [59–61].

Figure 8 shows the fractured surface morphology of unloaded and Pb(II)-loaded PC-PAAc/GA0 and PC-PAAc/GA1.5 hydrogels. From the FE-SEM micrographs, it is observed that minute voids are present on the surface that could facilitate the incorporation of the metal cation. As seen in Fig. 8b, d for the metal ions loaded hydrogels, the Pb(II) ions have adhered to the surface of the hydrogel matrix. It is also clear that all the hydrogels depict three-dimensional micro-porous inner structures. The porous structure plays a crucial role in water permeation regions to allow the penetration of aqueous solution containing the metal cation, owing to the absorption of water caused by the electrostatic forces resulting from the reactive groups within the polymer chains.

The effect of the initial Pb(II) ions concentration on the removal percentage is shown in Fig. 9a. It can be observed that the Pb(II) removal parentage decreases with increasing the initial metal ions concentration. At a low concentration of Pb(II), the vacant active sites on the hydrogel surface permit to adsorb more Pb(II) ions. By increasing the initial metal ions concentration, a decrease in the free active sites available for adsorption. This means a district of the free active sites required for adsorption thus decreasing the removal percentage of Pb(II) ions.

To know the possibility of interaction between PC-PAAc/GA hydrogels and Pb(II) the adsorption isotherms were studied [62].The adsorption isotherms express the heterogeneity/homogeneity of adsorbents [63]. For this purpose, the Langmuir and the Freundlich isotherm models were applied. The Langmuir model considers the monolayer adsorption of solutes onto definite sites on the adsorbent surface. No additional sorption can be done once these sites become filled. The isotherm model is presented by the following Eq. (3)

$$q_e = \frac{q_m K_L C_e}{1 + K_L C_e} \tag{3}$$

where C_e (mg/L) and q_e (mg/g) are the adsorbate concentration and the amount of adsorbates adsorbed at the equilibrium, respectively. K_L is the Langmuir constant (L/mg) and q_m the maximum adsorption capacity of the adsorbent (mg/g).

The Freundlich model considers the adsorption processes performed on a heterogonous surface.

The isotherm model is presented by the following Eq. (4)

$$q_e = K_F C_e^{1/n} \tag{4}$$

where K_F is the Freundlich isotherm constants and n is the adsorption intensity.

The two isotherm models are applied as shown in (Fig. 9b, c). It was found that the correlation coefficients of

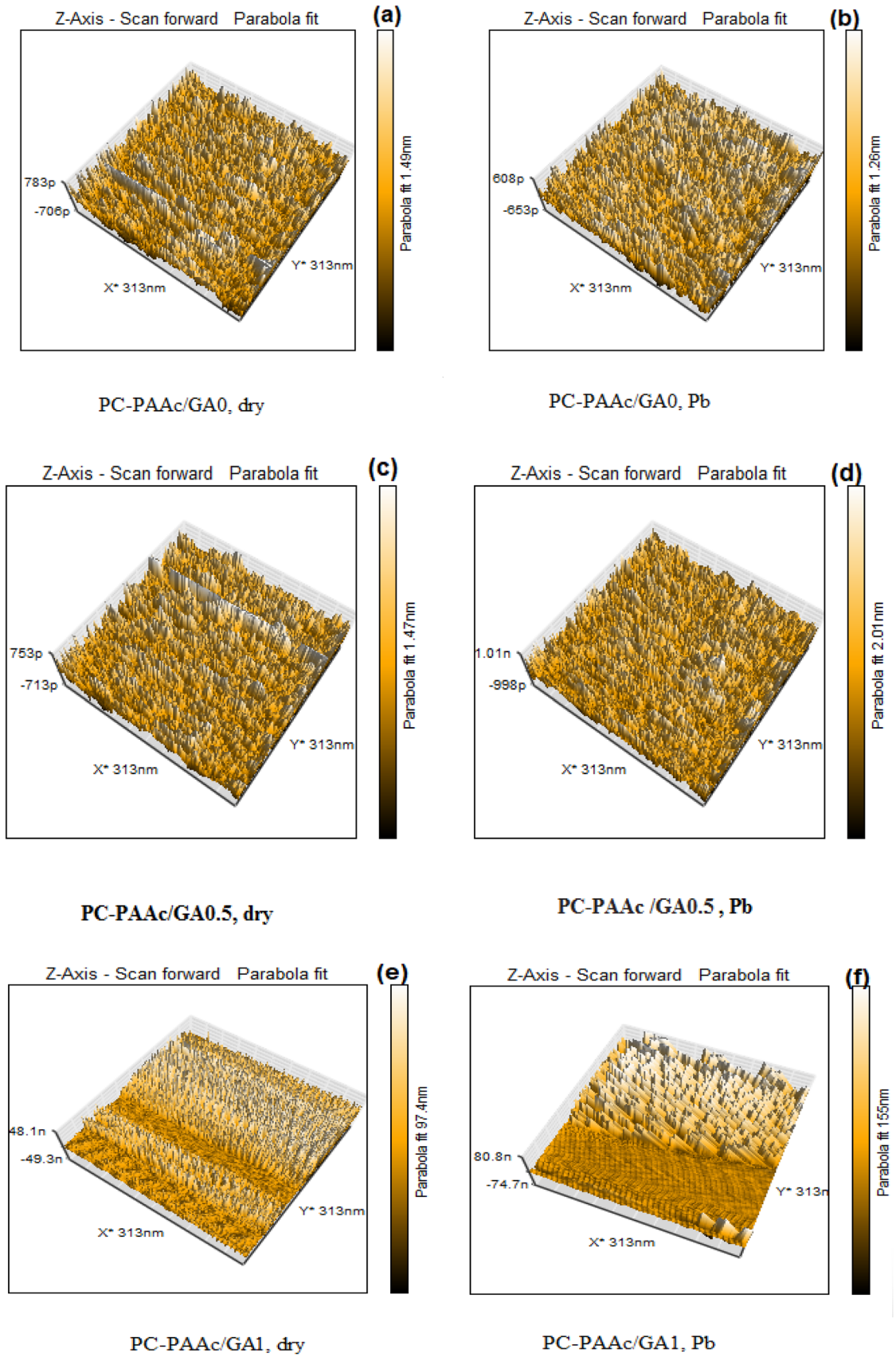

Fig. 7 AFM images (**a**-**j**), height data (**k**) and roughness data (**l**) of PC-PAAc/GA hydrogels after loading of Pb(II)

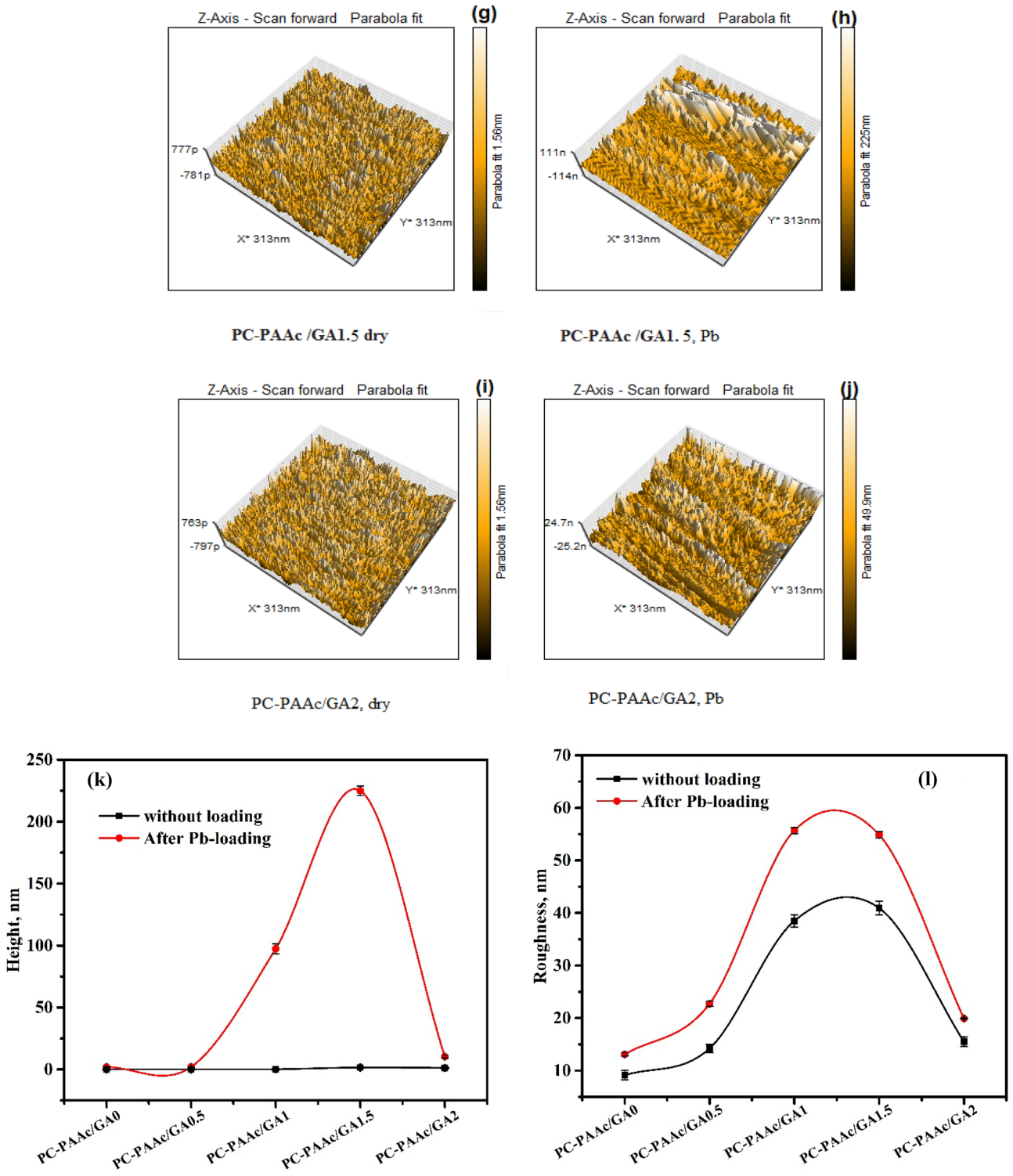

Fig. 7 (continued)

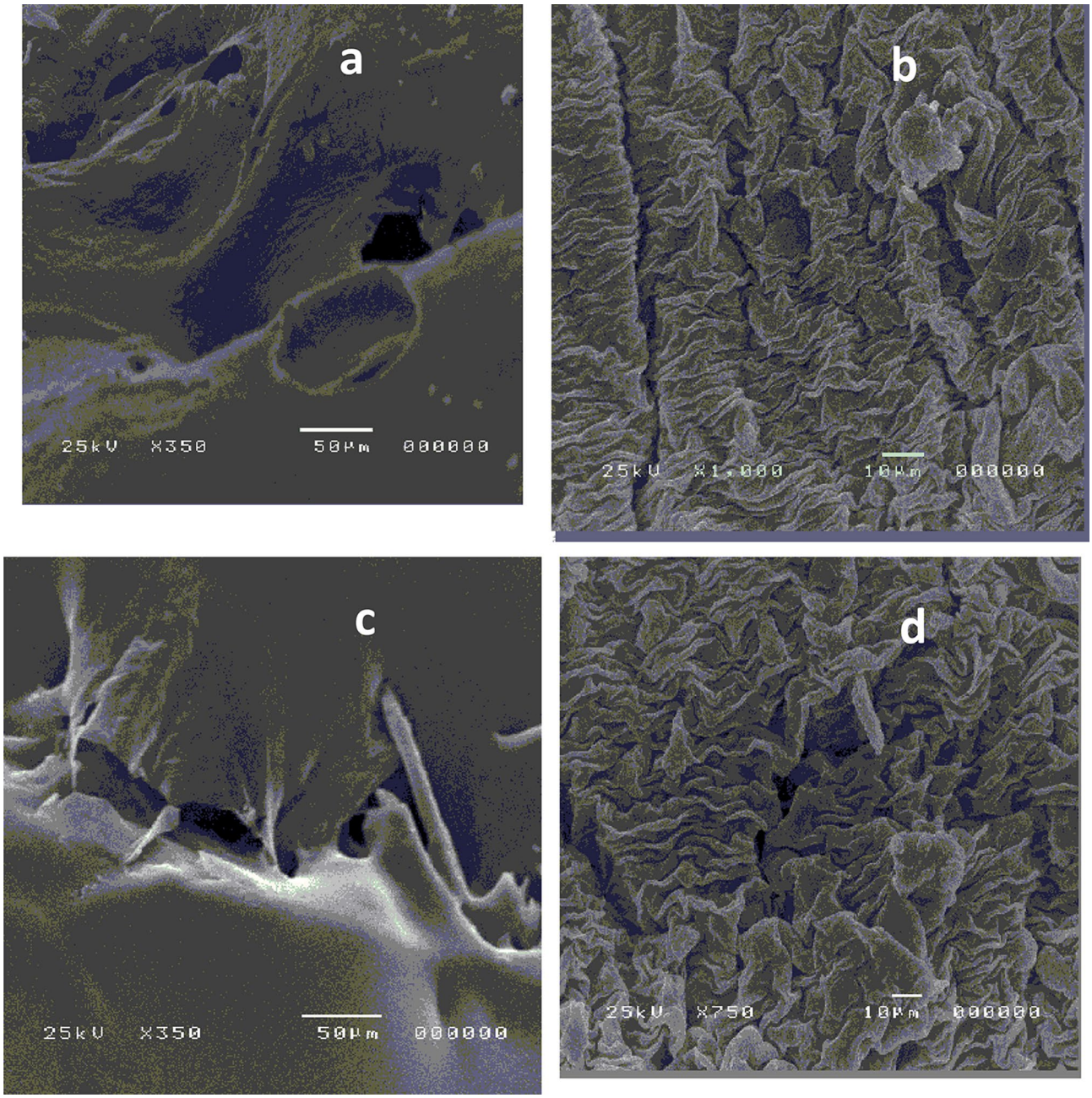

Fig. 8 FE-SEM of PC-PAAc/GA0 (**a**), Pb(II)- loaded PC-PAAc/GA0 (**b**), PC-PAAc/GA1.5 (**c**) and Pb(II)- loaded PC-PAAc/GA1.5 (**d**)

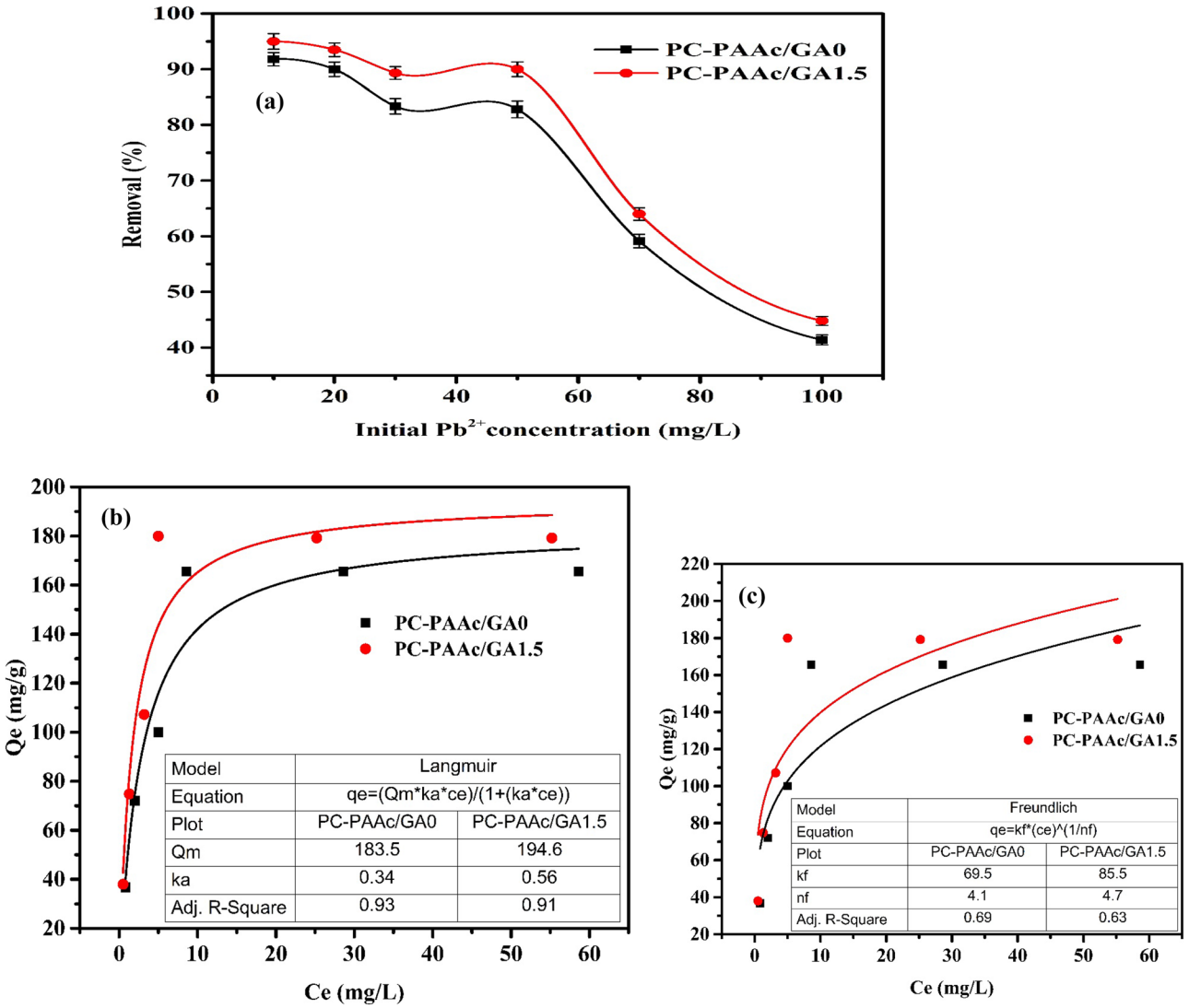

Fig. 9 Effect of initial Pb (II) concentration on removal (%) of PC-PAAc/GA hydrogel (**a**) Adsorption isotherms of Langmuir (**b**), and Freundlich (**c**) models; at room temperature, time 24 h and adsorbate weight 0.05 g

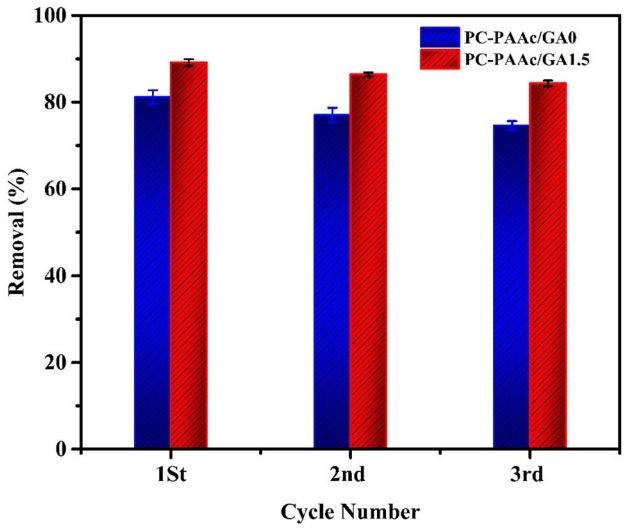

Fig. 10 Removal percentage (%) after three adsorption/desorption cycles of Pd^{2+}ions by PC-PAAc/GA0 and PC-PAAc/GA1.5 hydrogels initial Pd^{2+}ions conc. 50 mg/L

the Langmuir model are too higher than that of the Freundlich model for both PC-PAAc/GA0 and PC-PAAc/GA1.5 hydrogels. The results suggested that the active sites on the hydrogel surface are homogenously distributed. The adsorption of Pb(II) ions by PC-PAAc/GA hydrogel is a chemical adsorption process [64]. It is also noted that PC-PAAc/GA hydrogel contains many hydroxyl and carboxylic groups that can attract and coordinate with Pb (II) cations. A comparison between the removal performance of PC-PAAc/GA hydrogel and relevant formulations is given in Table 2.

The recyclability of the optimum hydrogel was conducted at three adsorption/desorption cycles and it was also compared with the hydrogel lacking GA, (Fig. 10). It was demonstrated that the removal performance is nearly the same with a negligible decline. This proves that the prepared sorbents can be used several times with an acceptable efficiency.

Table 2 A comparison between the removal performance of PC-PAAc/GA hydrogel and relevant formulations

Adsorbent	Adsorption capacity	Adsorption model	References
Sodium Alginate / Itaconic Acid	1.23 mmol/g	Freundlich	[65]
hydroxyapatite/polyacrylamide (HAp/PAAm) composite hydrogels	123–209 mg/g	Langmuir	[66]
Graphene oxide-chitosan-poly(acrylic acid) (GO-CS-AA) hydrogel nanocomposite	(138.89 mg g^{-1})	Langmuir	[67]
Hydrous ferric oxide-Poly(trans-aconitic acid/2-hydroxyethyl acrylate (HFO-P(TAA/HEA)) hydrogel	1.466 mmol/g	Langmuir	[68]
PC-PAAc/GA	90 mg/g	Langmuir	This work

Conclusion

Green hydrogels comprised of Pectin/polyacrylic acid/ gallic acid were prepared by using varying gallic acid content via gamma radiation at irradiation dose 20 kGy. The experimental data revealed that the hydrogel of formulation PC-PAAc/GA1.5 displayed the highest swelling capacity. The equilibrium of swelling was attained after 350 min and it was enhanced by increasing pH from 2 to 10. XRD analysis confirmed the amorphous structure of the hydrogels. TGA confirmed an improvement in the thermal stability by adding GA in the matrix. The results proved that the incorporation of GA in the hydrogel matrix resulted in excellent antibacterial activity against gram + bacteria *(E.coli)* and gram- bacteria *(S. aureus)*. The maximum removal percentage of Pb(II) by PC-PAAc/GA hydrogel is 90 mg g^{-1}. The correlation coefficients of the Langmuir model are too higher than that of the Freundlich model that assumed the adsorption is a chemical process.

Funding Open access funding provided by The Science, Technology & Innovation Funding Authority (STDF) in cooperation with The Egyptian Knowledge Bank (EKB).

Data availability statement The raw data supporting the conclusions of this article will be made available by the authors, without undue reservation.

Declarations

Competing interests The authors declare that they have no known competing financial interests or personal relationships that could have appeared to influence the work reported in this paper.

References

1. Sayan B et al (2013) Role of nanotechnology in water treatment and purification: potential applications and implications. Int J Chem Sci Technol 3(3):59

2. Khozamy E et al (2019) Implementation of carboxymethyl cellulose/acrylic acid/titanium dioxide nanocomposite hydrogel in remediation of Cd (II), Zn (II) and Pb (II) for water treatment application. Egypt J Chem 62(10):1785–1798
3. Elshahawy MF et al (2020) Fabrication of TiO2 reduced graphene oxide based nanocomposites for effective of photocatalytic decolorization of dye effluent. J Inorg Organomet Polym Mater 30(7):2720–2735
4. Raafat AI, Mahmoud GA, Mostafa TB (2020) Efficient catalytic reduction of hazardous anthropogenic pollutant, 4-nitrophenol using radiation synthesized (polyvinyl pyrrolidone/acrylic acid)-silver nanocomposite hydrogels. J Inorg Organomet Polym Mater 30(8):3116–3125
5. Kumar V et al (2022) Synthesis and characterization of Aloe-vera-poly (acrylic acid)-Cu-Ni-bionanocomposite: its evaluation as removal of carcinogenic dye malachite green. J Polym Res 29(2):1–14
6. Owa F (2013) Water pollution: sources, effects, control and management. Mediterr J Soc Sci 4(8):65–65
7. Amin MTK (2020) Chitosan biopolymer based nanocomposite hydrogels for removal of methylene blue dye
8. Gaur N et al (2014) A review with recent advancements on bioremediation-based abolition of heavy metals. Environ Sci Process Impacts 16(2):180–193
9. Masindi V, Muedi KL (2018) Environmental contamination by heavy metals. Heavy metals 10:115–132
10. Mahmoud ME, Mohamed AK (2020) Novel derived pectin hydrogel from mandarin peel based metal-organic frameworks composite for enhanced Cr (VI) and Pb (II) ions removal. Int J Biol Macromol 164:920–931
11. Liu P et al (2014) Cellulose and chitin nanomaterials for capturing silver ions (Ag+) from water via surface adsorption. Cellulose 21(1):449–461
12. Vijayaraghavan K, Palanivelu K, Velan M (2006) Biosorption of copper (II) and cobalt (II) from aqueous solutions by crab shell particles. Biores Technol 97(12):1411–1419
13. Liu P, Oksman K, Mathew AP (2016) Surface adsorption and self-assembly of Cu (II) ions on TEMPO-oxidized cellulose nanofibers in aqueous media. J Colloid Interface Sci 464:175–182
14. Ali AE-H et al (2016) Photocatalytic decolorization of dye effluent using radiation developed polymeric nanocomposites. J Inorg Organomet Polym Mater 26(3):606–615
15. Barakat M, Schmidt E (2010) Polymer-enhanced ultrafiltration process for heavy metals removal from industrial wastewater. Desalination 256(1–3):90–93
16. Mahmoud GA, Ezz El-Din MR, Mohamed AA (2021) Safe isolation and storage of simulated radioactive waste contains cesium and cobalt ions by magnetic natural-based nanocomposites. Polym Bull 1–18
17. Abdulghany AH et al (2021) A biodegradable based composite for wastewater treatment from cadmium and nickel ions. Desalin Water Treat 223:316–327
18. Chen J et al (2020) Preparation of a hydrogel-based adsorbent for metal ions through high internal phase emulsion polymerization. ACS Omega 5(32):19920–19927
19. Yao Q et al (2014) Adsorption of lead ions using a modified lignin hydrogel. J Polym Res 21(6):1–16
20. Mahmoud GA et al (2016) Radiation synthesis of imprinted hydrogels for selective metal ions adsorption. Desalin Water Treat 57(35):16540–16551
21. Khozemy EE, Nasef SM, Mahmoud GA (2018) Synthesis and characterization of antimicrobial nanocomposite hydrogel based on wheat flour and poly (vinyl alcohol) using γ-irradiation. Adv Polym Technol 37(8):3252–3261
22. Mohamed AA et al (2020) Synthesis and properties of (Gum acacia/polyacryamide/SiO2) magnetic hydrogel nanocomposite prepared by gamma irradiation. Polym-Plast Technol Mater 59(4):357–370
23. Rattanawongwiboon T et al (2020) Chitosan-poly (ethylene glycol) diacrylate beads prepared by radiation-induced crosslinking and their promising applications derived from encapsulation of essential oils. Radiat Phys Chem 170:108656
24. Silva AC et al (2022) Natural polymers-based materials: A contribution to a greener future. Molecules 27(1):94
25. Doppalapudi S et al (2015) Biodegradable natural polymers. Adv Polym Med. Springer, pp 33–66
26. Mahmoud GA et al (2018) Characterization and properties of magnetic and non-magnetic (Gum Acacia/Polyacryamide/Graphene) nanocomposites prepared by gamma irradiation. J Inorg Organomet Polym Mater 28(6):2633–2644
27. El-Fadl F et al (2017) Pectin-based hydrogels and its ferrite nanocomposites for removal of nitro compounds. Desalin Water Treat 90:283–293
28. Babaladimath G, Badalamoole V (2018) Pectin-graft-poly (2-acrylamido-2-methyl-1-propane sulfonic acid) silver nanocomposite hydrogel beads: evaluation as matrix material for sustained release formulations of ketoprofen and antibacterial assay. J Polym Res 25(9):1–12
29. Suksaeree J et al (2018) Use of isolated pectin from a Cissampelos pareira-based polymer blend matrix for the transdermal delivery of nicotine. J Polym Environ 26(9):3531–3539
30. Kodoth AK, Badalamoole V (2019) Pectin based graft copolymer–ZnO hybrid nanocomposite for the adsorptive removal of crystal violet. J Polym Environ 27(9):2040–2053
31. Chen D et al (2021) Pectin-based self-healing hydrogel with NaHCO3 degradability for drug loading and release. J Polym Res 28(2):1–10
32. Ali L et al (2020) Cross-linked pH-sensitive pectin and acrylic acid based hydrogels for controlled delivery of metformin. Pak J Pharm Sci 33(4)
33. Mahmoud GA et al (2017) A novel hydrogel based on agricultural waste for removal of hazardous dyes from aqueous solution and reuse process in a secondary adsorption. Polym Bull 74(2):337–358
34. Fares MM et al (2011) Eco-friendly, vascular shape and interpenetrating poly (acrylic acid) grafted pectin hydrogels; biosorption and desorption investigations. J Polym Environ 19(2):431–439
35. Badhani B, Sharma N, Kakkar R (2015) Gallic acid: a versatile antioxidant with promising therapeutic and industrial applications. RSC Adv 5(35):27540–27557
36. Han D et al (2011) Preparation of chitosan/graphene oxide composite film with enhanced mechanical strength in the wet state. Carbohyd Polym 83(2):653–658
37. Mahmoud GA et al (2014) Radiation synthesis and characterization of starch-based hydrogels for removal of acid dye. Starch-Stärke 66(3–4):400–408
38. Zhen SJ (2003) Radiation crosslinking of polymer blend system: Radiation degradative polymer blended with radiation crosslinking polymer. Radiat Technol Emerg Ind Appl 2
39. Chmielewski AG, Haji-Saeid M, Ahmed S (2005) Progress in radiation processing of polymers. Nucl Instrum Methods Phys Res Sect B 236(1–4):44–54
40. Mahmoud GA et al (2014) Characterisation of alginate-based nanocomposites prepared by radiation for removal of pesticides. Int J Nanoparticles 7(3–4):213–230
41. El-Kelesh NA, Mahmoud GA (2015) Synthesis and properties of treated waste cellulose and GMA grafted composite to remove different acid dyes from aqueous solutions. Cellul Chem Technol 49:881–889
42. Chang M et al (2021) Mussel-inspired adhesive hydrogels based on biomass-derived xylan and tannic acid cross-linked with acrylic acid with antioxidant and antibacterial properties. J Mater Sci 56(26):14729–14740
43. Sayed A et al (2022) Characterization and optimization of magnetic Gum-PVP/SiO2 nanocomposite hydrogel for removal of contaminated dyes. Mater Chem Phys 125731

44. Manas D et al (2018) The effect of irradiation on mechanical and thermal properties of selected types of polymers. Polymers 10(2):158
45. Gehring J, Zyball A (1995) Radiation crosslinking of polymers-status, current issues, trends and challenges. Radiat Phys Chem 46(4–6):931–936
46. Makuuchi K, Cheng S (2012) Radiation processing of polymer materials and its industrial applications. John Wiley & Sons
47. Zhang J et al (2007) Dual thermo-and pH-sensitive poly (N-isopropylacrylamide-co-acrylic acid) hydrogels with rapid response behaviors. Polymer 48(6):1718–1728
48. Peng X-W et al (2011) Xylan-rich hemicelluloses-graft-acrylic acid ionic hydrogels with rapid responses to pH, salt, and organic solvents. J Agric Food Chem 59(15):8208–8215
49. Radwan RR et al (2018) Radiation preparation of l-arginine/acrylic acid hydrogel matrix patch for transdermal delivery of propranolol HCl in hypertensive rats. Drug Deliv Transl Res 8(3):525–535
50. Neo YP et al (2013) Encapsulation of food grade antioxidant in natural biopolymer by electrospinning technique: A physicochemical study based on zein–gallic acid system. Food Chem 136(2):1013–1021
51. Meenakshi S et al (2009) Total flavanoid and in vitro antioxidant activity of two seaweeds of Rameshwaram coast. Glob J Pharmacol 3(2):59–62
52. Ranjha NM, Mudassir J, Zubair SZ (2011) Synthesis and characterization of pH-sensitive pectin/acrylic acid hydrogels for verapamil release study
53. Giubertoni G, Sofronov OO, Bakker HJ (2020) Effect of intramolecular hydrogen-bond formation on the molecular conformation of amino acids. Commun Chem 3(1):1–6
54. Dafe A et al (2017) Investigation of pectin/starch hydrogel as a carrier for oral delivery of probiotic bacteria. Int J Biol Macromol 97:536–543
55. Samper M et al (2013) The potential of flavonoids as natural antioxidants and UV light stabilizers for polypropylene. J Appl Polym Sci 129(4):1707–1716
56. Dopico-García M et al (2011) Natural extracts as potential source of antioxidants to stabilize polyolefins. J Appl Polym Sci 119(6):3553–3559
57. Miklasińska-Majdanik M et al (2018) Phenolic compounds diminish antibiotic resistance of Staphylococcus aureus clinical strains. Int J Environ Res Public Health 15(10):2321
58. Shakeri A et al (2012) Removal of lead (ii) from aqueous solution using cocopeat: an investigation on the isotherm and kinetic
59. Zhang X et al (2010) Chemical cross-linking gelatin with natural phenolic compounds as studied by high-resolution NMR spectroscopy. Biomacromol 11(4):1125–1132
60. Gray KM et al (2011) Biomimetic fabrication of information-rich phenolic-chitosan films. Soft Matter 7(20):9601–9615
61. Hasan AM, Keshawy M, Abdel-Raouf ME-S (2022) Atomic force microscopy investigation of smart superabsorbent hydrogels based on carboxymethyl guar gum: Surface topography and swelling properties. Mater Chem Phys 278:125521
62. Abbar B et al (2017) Experimental investigation on removal of heavy metals (Cu2+, Pb2+, and Zn2+) from aqueous solution by flax fibres. Process Saf Environ Prot 109:639–647
63. Al-Gorair AS, Sayed A, Mahmoud GA (2022) Engineered superabsorbent nanocomposite reinforced with cellulose nanocrystals for remediation of basic dyes: Isotherm, kinetic, and thermodynamic studies. Polymers 14(3):567
64. Zhang W et al (2019) Optimized synthesis of novel hydrogel for the adsorption of copper and cobalt ions in wastewater. RSC Adv 9(28):16058–16068
65. Mahmoud GA, Mohamed SF (2012) Removal of lead ions from aqueous solution using (sodium alginate/itaconic acid) hydrogel prepared by gamma radiation. Aust J Basic Appl Sci 6(6):262–273
66. Jang SH et al (2008) Preparation and lead ion removal property of hydroxyapatite/polyacrylamide composite hydrogels. J Hazard Mater 159(2–3):294–299
67. Medina RP et al (2016) Incorporation of graphene oxide into a chitosan–poly (acrylic acid) porous polymer nanocomposite for enhanced lead adsorption. Environ Sci Nano 3(3):638–646
68. Zhang Y, Li Z (2017) Heavy metals removal using hydrogel-supported nanosized hydrous ferric oxide: Synthesis, characterization, and mechanism. Sci Total Environ 580:776–786